Biology of Reproduction, 2017, 97(1), 18–31
doi:10.1093/biolre/iox059
Research Article
Advance Access Publication Date: 19 June 2017

Research Article

The transcriptome of the endometrium and placenta is associated with pregnancy development but not lactation status in dairy cows†,‡

Stephen G. Moore[1], Matthew S. McCabe[2], Jacob C. Green[1], Emily M. Newsom[1] and Matthew C. Lucy[1,*]

[1]Division of Animal Sciences, University of Missouri, 160 Animal Science Research Center, Columbia, Missouri, USA and [2]Animal and Bioscience Research Department, Animal and Grassland research and Innovation Centre, Teagasc, Grange, Dunsany, Co. Meath, Ireland

*__Correspondence:__ Division of Animal Sciences, 160 Animal Science Research and Innovation Center, 920 East Campus Drive, University of Missouri, Columbia, MO 65211, USA. E-mail: lucym@missouri.edu

†__Grant Support:__ This research was supported by the University of Missouri Experiment Station, the Food for the 21st Century program of the University of Missouri and Pfizer Animal Health (Kalamazoo, MI).
‡Raw CEL files were deposited in the NCBI Gene Expression Omnibus (accession number: GSE94794).
__Conference Presentation:__ Part of this research was presented at the International Congress of Animal Reproduction, June 26–30 2016, Tours, France.

Received 10 February 2017; Revised 7 June 2017; Accepted 17 June 2017

Abstract

Infertility in lactating dairy cows is explained partially by the metabolic state associated with high milk production. The hypothesis was that lactating and nonlactating cows would differ in endometrial and placental transcriptomes during early pregnancy (day 28 to 42) and this difference would explain the predisposition for lactating cows to have embryonic loss at that time. Cows were either milked or not milked after calving. Reproductive [endometrium (caruncular and intercaruncular) and placenta] and liver tissues were collected on day 28, 35, and 42 of pregnancy. The hypothesis was rejected because no effect of lactation on mRNA abundance within reproductive tissues was found. Large differences within liver demonstrated the utility of the model to test an effect of lactation on tissue gene expression. Major changes in gene expression in reproductive tissues across time were found. Greater activation of the transcriptome for the recruitment and activation of macrophages was found in the endometrium and placenta. Changes in glucose metabolism between day 28 and 42 included greater mRNA abundance of rate-limiting genes for gluconeogenesis in intercaruncular endometrium and evidence for the establishment of aerobic glycolysis (Warburg effect) in the placenta. Temporal changes were predicted to be controlled by *CSF1*, *PDGFB*, *TGFB1*, and *JUN*. Production of nitric oxide and reactive oxygen species by macrophages was identified as a mechanism to promote angiogenesis in the endometrium. Reported differences in pregnancy development for lactating vs. nonlactating cows could be explained by systemic glucose availability to the conceptus and appeared to be independent of the endometrial and placental transcriptomes.

Summary Sentence

Expression of genes in the pregnant bovine uterus is not affected by lactation.

Key words: endometrium, placenta, liver, lactation, pregnancy.

Introduction

Mechanisms leading to poor fertility in lactating dairy cows are intensely studied because of the global decline in dairy cow fertility since the 1950's. Although fertility decline reached a nadir recently and fertility now appears to be trending upward [1], reproductive efficiency of lactating cows is still problematic. In confinement systems, for example, hormonal interventions are widely used to establish pregnancies efficiently. In seasonal dairy systems that do not use hormonal intervention, 10 to 20% of cows are not pregnant at the end of the breeding season. Approximately 85% of oocytes are successfully fertilized after insemination and presumably a viable zygote is present. Less than half of these zygotes, however, develop to term because of high rates of embryonic loss in dairy cows. At least two periods of pregnancy loss have been described based on the availability of pregnancy diagnosis data [2]. The first period of pregnancy loss equates to 20 to 40% during the first 28 days of gestation. This first period of pregnancy loss involves the cleavage stage and filamentous embryos. Although studying embryonic loss during this period is difficult, some mechanisms of pregnancy loss have been elucidated [2,3]. The second period of pregnancy loss from days 28 to 60 of gestation accounts for less loss (approximately 5 to 25%) and is easier to study because embryonic death can be measured by ultrasound [2]. The second period coincides with the establishment and growth of the placenta and the completion of conceptus attachment to the uterus. Although the overall percentages are less, the second period of pregnancy loss is viewed with greater concern because it occurs later during gestation (greater time committed to the pregnancy) and cows are initially diagnosed pregnant on farm but later found to be not pregnant after a second ultrasound exam [4,5]. Regardless of when they occur, pregnancy losses reduce farm productivity and profitability and threaten food security.

A defining characteristic of the early postpartum dairy cow is her capacity to undergo nutrient partitioning to support the production of milk [6]. High milk production and metabolic imbalance associated with nutrient partitioning have been implicated as factors responsible for suboptimal reproductive performance [7,8]. Suboptimal reproductive performance is in part explained by embryonic loss during both periods. We hypothesized that lactation would negatively affect the rate of fetal development during the second period of embryonic loss through mechanisms involving differential gene expression. To examine this hypothesis, we designed an experiment in which postpartum cows were assigned to one of two treatments immediately after parturition [lactating or nonlactating (dried off immediately after calving)] and had their pregnancies collected on day 28, 35, or 42 of gestation. The effects of lactation on the metabolic profiles of the cattle and the pregnancy itself were reported previously [9]. Lactating cows had inferior metabolic status [9,10], later resumption of ovarian cyclicity [10], lesser placental fluid glucose and fructose concentrations [11] and lesser fetal and placenta weights [9] from day 28 to 42 of gestation. The slower fetal and placental development may predispose lactating cows to pregnancy loss if developmental milestones are not reached. Others followed this initial work with additional postpartum dairy cows that were either lactating or nonlactating and have found similar rates of uterine involution [12] but a suboptimal immune- and development-related endometrial expression profile on day 17 of pregnancy [13]. In the current study, we examined the transcriptome of the endometrium and placenta in samples collected on day 28, 35, and 42 of gestation from the same cows used in the Green et al. (2012) study [9]. We hypothesized that the differences in lactation status (i.e., lactating vs. nonlactating) would affect the transcriptome of the endometrium and placenta and may explain their previously reported differences in pregnancy development [9].

Materials and methods

Animal model

The animal model used in the present study has previously been described [9]. The project was approved by the University of Missouri-Columbia Animal Care and Use Committee. Cows were housed at the University of Missouri-Columbia Foremost Dairy Farm. Pregnant *Bos taurus* Holstein heifers (n = 43) were assigned to one to two treatment groups based on calving date (alternating between treatments): lactating (n = 23) and not lactating (n = 20). There were two groups of cows. The first group (n = 21) calved from March to July, and the second group (n = 22) calved from September to December.

Animal management

After calving, the lactating cows were milked twice daily and the nonlactating cows were not milked (i.e., dried off immediately, never milked). Both groups of cows were housed together in a two-row freestall barn. The freestalls were sand-bedded, and there was a solid concrete floor. A diet consisting of corn silage, alfalfa haylage, grass hay, concentrates, and minerals was provided with equal access via bunk feeding for both groups of cows.

Ovarian morphology [corpora lutea and follicles ≥5 mm] was recorded weekly using transrectal ultrasonography (Aloka 500-SSD equipped with 7.5 MHz transducer, Aloka, Tokyo, Japan). Both lactating and nonlactating cows were enrolled in an ovulation synchronization protocol (Presynch–Ovsynch) so that the first artificial insemination occurred from 56 to 62 days postpartum. For the Presynch component, each cow was administered an i.m. injection of $PGF_{2\alpha}$ containing 25 mg dinoprost tromethamine (Lutalyse; Zoetis, New York, NY, USA) on days −36 and −22 relative to artificial insemination. The Ovsynch component began on day −10 relative to artificial insemination. Each cow was administered an i.m. injection of GnRH containing 100 mg of gonadorelin hydrochloride (Factrel; Zoetis). On day −3, each cow was administered an i.m. injection of $PGF_{2\alpha}$ containing 25 mg dinoprost tromethamine. Fifty-six hours later, each cow was administered an i.m. injection of GnRH (100 mg of gonadorelin hydrochloride). Sixteen hours later, each cow was submitted for artificial insemination. Three lactating cows and two nonlactating cows without a corpus luteum at the time of administration of the first GnRH injection (day −10 relative to artificial insemination) were administered, one controlled internal drug release (CIDR; Zoetis) containing 1.38 g of progesterone per vaginum for 7 days. Each device was removed at the time of $PGF_{2\alpha}$ injection (day −3 relative to artificial insemination). Each cow was

inseminated from a single ejaculate of a high fertility sire (Regancrest-RB Miles, 7HO7037; Select Sires, Plain City, OH, USA). Cows that did not conceive at first insemination were inseminated 12 h after an observed return to estrus using semen from the same sire and ejaculate as used for the first artificial insemination. Cows not pregnant to the first artificial insemination and not observed in estrus were resynchronized for timed artificial insemination using the Ovsynch protocol just described. Pregnancy was diagnosed using transrectal ultrasonography and by using an enzyme-linked immunosorbent assay for pregnancy-associated glycoproteins [14].

Tissue collection

Pregnant cows were slaughtered at either day 28 (n: lactating = 7, nonlactating = 7; 105 ± 28 days postpartum), day 35 (n: lactating = 8, nonlactating = 6; 108 ± 29 days postpartum), or day 42 (n: lactating = 8, nonlactating = 7; 114 ± 13 days postpartum) within 2 h after the morning milking. Cows were stunned by using a pneumatic captive bolt and then killed by exsanguination. The reproductive tracts and a liver sample were collected, placed on crushed ice and taken to the laboratory within 30 min of slaughter. The pregnancy (placental membranes encasing placental fluids and fetuses) was removed from the uterus. The placental fluids (mixture of both amniotic and allantoic fluids) were collected and a sample frozen at –80°C. Samples of caruncular endometrium, intercaruncular endometrium, and all of the placental membranes were frozen in liquid nitrogen so that they could be used for RNA analysis. For endometrial tissue collection (caruncular and intercaruncular endometrium), five to ten representative 1 cm × 1 cm samples interspaced along the pregnant horn were collected from each region, frozen in liquid nitrogen, and stored at –80°C. The five to ten individual tissue samples within each tissue type from each cow were later combined and ground together under liquid nitrogen with a mortar and pestle. Total cellular RNA was isolated by using the TRIzol reagent (Invitrogen; Carlsbad, CA). Caruncular endometrium and intercaruncular endometrium samples were further purified by using the QIAmp Mini Spin Column (Qiagen, Valencia, CA). The integrity of RNA was determined by visual inspection of 28S and 18S RNA bands after agarose gel electrophoresis and by calculating the ratio of absorbance at 260 and 280 nm. The RNA that was used had intact 28S and 18S RNA bands, and the 260:280 nm ratio was greater than 1.8. The RNA was diluted in water and stored at –80°C. The DNA core facility at the University of Missouri subsequently performed their own independent quality control of the RNA samples using an Agilent Bioanalyzer 2100 (Agilent Technologies, Inc., Santa Clara, CA) prior to its use in the microarray assay.

Microarray hybridization and analysis

The DNA core facility at the University of Missouri performed the microarray assay. Total RNA (0.5 μg) was used to make the biotin-labeled antisense RNA (aRNA) target using the MessageAmp Premier RNA amplification kit (Ambion, Austin, TX) by following the manufacturer's procedures. Briefly, the total RNA was reverse transcribed to first-strand cDNA with an oligo(dT) primer bearing a 5'-T7 promoter using ArrayScript reverse transcriptase (Ambion). The first-strand cDNA then underwent second-strand synthesis to convert into double-stranded cDNA template for in vitro transcription. The biotin-labeled aRNA was synthesized using T7 RNA transcriptase with biotin-NTP mix. After purification, the aRNA was fragmented in fragmentation buffer at 94°C for 35 min. One hundred thirty microliter of hybridization solution containing 50 ng/μl of fragmented aRNA was hybridized to the Bovine Genome Array Genechip (Affymetrix, Santa Clara, CA) at 45°C for 20 h. The Bovine Genome Array utilizes content from Bovine UniGene Build 57 (March 24, 2004) and GenBank mRNAs. After hybridization, the chips were washed and stained with R-phycoerythrin-streptavidin on Affymetrix fluidics station 450 using fluidics protocol Midi_euk2v3–450. The image data were acquired by Affymetrix Genechip scanner 3000.

Differential analysis of gene expression

Two cows were excluded from the analysis. One lactating cow slaughtered on day 28 had no pregnancy present and one nonlactating cow slaughtered on day 42 had a nonviable pregnancy assessed by the poor vascular development and detachment of the placenta from the uterine wall. Differential expression analysis of the liver, intercaruncular endometrium, caruncular endometrium, and placenta tissue microarray data was performed separately using the Bioconductor software package limma [15] with the R statistical programming language (version 3.2.2) [16]. The Gene Chip Robust Multi-array package was used to convert background adjusted probe intensities of each CEL file to an expression measure [17]. Array quality metrics were assessed using the arrayQualityMetrics package [18]. Principal component analysis is illustrated in Supplementary Figure S1. The data were filtered to remove control probesets (n = 112). For the differential expression analysis within tissue, a linear model was fitted to the expression data for each probe with lactation status (lactating, nonlactating), group (one, two), day of gestation (28, 35, 42), and their interactions included as fixed effects. For the differential expression analysis between caruncular and intercaruncular tissue, the linear model included tissue (caruncular endometrium, intercaruncular endometrium), day of gestation (28, 35, 42), and their interaction as fixed effects and cow as a random effect. For each analysis, the limma package applies empirical Bayes methods to compute moderated t-tests. Transcripts were deemed differentially expressed at $P \leq 0.01$ after adjustment for multiple testing using the Benjamini and Hochberg (BH) method [19].

Real-time RT-PCR validation of microarray data

Total RNA was transcribed into cDNA by using the High Capacity cDNA Reverse Transcription Kit (Applied Biosystems, Foster City, CA). Quantitative reverse transcription polymerase chain reaction (RT-PCR) was used to assay the amount of cDNA (i.e., mRNA) in each sample. The reaction was performed in an ABI Prism 7700 machine (Applied Biosystems) using the QuantiTect SYBR Green PCR Kit (Qiagen) and primers that were specific for RNA transcripts (Supplementary Table S1). The PCR products produced from the RT-PCR were DNA sequenced to verify amplification of the target sequence. Within each plate there were high, medium, and low control samples (sequential 1:4 dilutions) of pooled cDNA that were run in triplicate. Each 96-well PCR plate contained a "no template control" (water substituted for cDNA in the reaction) to ensure that there was no amplification in samples without cDNA. Data from the serial dilutions of the control sample were used to calculate the amplification efficiencies for the RT-PCR (Supplementary Table S1) by using previously described procedures [20]. Fold change differences for the respective samples were calculated relative to an internal control standard within each plate according to previously described procedures [20]. Gene expression was initially assayed by using a single RT-PCR plate that included all of the cDNA samples in duplicate from a single tissue (liver, placenta, etc.). Data from individual tissues were analyzed by using the General Linear Models procedure (PROC GLM) of SAS (SAS Inst. Cary, North Carolina

Table 1. Summary of the number of differentially expressed genes in each tissue between lactating and nonlactating cows and between different days of gestation (35 vs. 28, 42 vs. 35, and 42 vs. 28).

Comparison		Intercaruncular endometrium	Caruncular endometrium	Placenta	Liver
Lactating vs. nonlactating cows	Increased expression	0	0	0	390
	Decreased expression	0	0	0	325
	Total	0	0	0	715
Day 35 vs. 28	Increased expression	284	18	193	0
	Decreased expression	649	27	202	0
	Total	933	45	395	0
Day 42 vs. 35	Increased expression	75	0	10	0
	Decreased expression	8	0	3	0
	Total	83	0	13	0
Day 42 vs. 28	Increased expression	1788	468	1029	0
	Decreased expression	2728	387	1367	0
	Total	4516	855	2396	0

USA) and tested for the effects of lactation status, group, day of gestation, group by lactation status, and group by day of gestation. Results are reported as least square means ± SEM.

Ingenuity Pathway Analysis and DAVID gene ontology analysis

Each dataset of differentially expressed probe sets was submitted separately in Ingenuity Pathway Analysis (IPA; Qiagen, Redwood City, CA, www.qiagen.com/ingenuity). From each dataset, a new dataset was generated with probes mapped only to a single gene retained. Each new dataset was submitted for Core analysis with the Affymetrix GeneChip Bovine Genome Array as the reference set to identify enriched canonical pathways (well-characterized metabolic and cell signaling pathways; deemed enriched at $P \leq 0.05$ and z-score [ZS] $\geq |2|$), biological functions, and predicted regulators of biological functions (both deemed significant at an overlap $P \leq 0.01$ and ZS $\geq |2|$). A ZS is a prediction of activation (>0) or inhibition (<0). Where applicable, possible relationships between regulators and biological functions were generated from prior biological knowledge using regulatory effects analysis. Regulator effect networks generate hypotheses connecting upstream regulators, dataset molecules, and biological functions. Hypotheses are generated for how a biological function is regulated in the dataset by activated or inhibited upstream regulators. The default setting was used which limited upstream regulators to genes, RNA, and proteins but did not limit the size of the network. Regulator effects networks with a positive consistency score (a measure of how causally consistent and densely connected a regulator effects network is) were deemed relevant. Gene ontology (GO) analysis of the differentially expressed genes in the liver, intercaruncular endometrium, caruncular endometrium, and placenta was performed using the Database for Annotation, Visualization and Integrated Discovery (DAVID) [21,22] for functional annotation. GO terms with BH-corrected *P*-values ≤ 0.05 were deemed significant.

Results

Summary of differential expression analysis in endometrium, placenta, and liver

The significant effects (BH corrected $P \leq 0.01$) of lactation status and day of gestation on the transcriptome of the endometrium, placenta, and liver are reported in Table 1. Differential expression analysis did not detect any differentially expressed genes in the endometrium or placenta for lactating vs. nonlactating cows sampled on day 28, 35, and 42 of gestation. Significant effects of lactation on mRNA abundance were detected in the liver with 715 differentially expressed genes between lactating and nonlactating cows (Supplementary Table S2). Day of gestation had a significant effect on mRNA abundance in the endometrium and placenta with 933, 83, and 4516 differentially expressed genes in intercaruncular endometrium (Supplementary Tables S3–S5); 45, 0, 855 differentially expressed genes in caruncular endometrium (Supplementary Tables S6–S7); and 395, 13, and 2396 differentially expressed genes in placenta (Supplementary Tables S8–S10) on day 28 vs. 35, day 35 vs. 42, and day 28 vs. 42, respectively. Significant differences in mRNA abundance between caruncular and intercaruncular endometrium were detected with 5232 differentially expressed genes (Supplementary Table S11). No significant interactions between lactation status and day of gestation on mRNA abundance were detected.

Comparison of endometrium tissues revealed that 727 of the 855 differentially expressed genes (85%) in the caruncular endometrium between day 28 and 42 of gestation were also differentially expressed in the intercaruncular endometrium. Linear regression of the expression profiles between the two tissues was high with an $r^2 = 0.84$ and a slope = 1.06 (Figure 1). Validation of select genes of interest from the analysis of the endometrium, placenta, and liver microarray data was performed by comparison with real-time RT-PCR testing (Supplementary Tables S12–S13). Twelve of the 16 endometrium and placenta genes, and 12 of the 14 liver genes were concordant at a minimum $P < 0.1$. Of the genes that were not validated by the real-time RT-PCR testing, their direction of expression (upregulation vs. downregulation) was in agreement (*ATF3*, *DEF5B*, *IGFBP2*, and *PRLR* in the caruncular endometrium and *CYP2C87* in the liver), except for *PRKAR1A*.

Differences in the liver transcriptome between lactating and nonlactating cows

Of the 715 transcripts differentially expressed (BH $P \leq 0.01$) in the liver between lactating and nonlactating cows (Supplementary Table S2), a dataset of 517 genes (221 upregulated and 296 downregulated in lactating cows) were retained for IPA. Canonical pathways in liver tissue were not significantly affected by lactation status. Downstream effects analysis (Supplementary Table S14) predicted

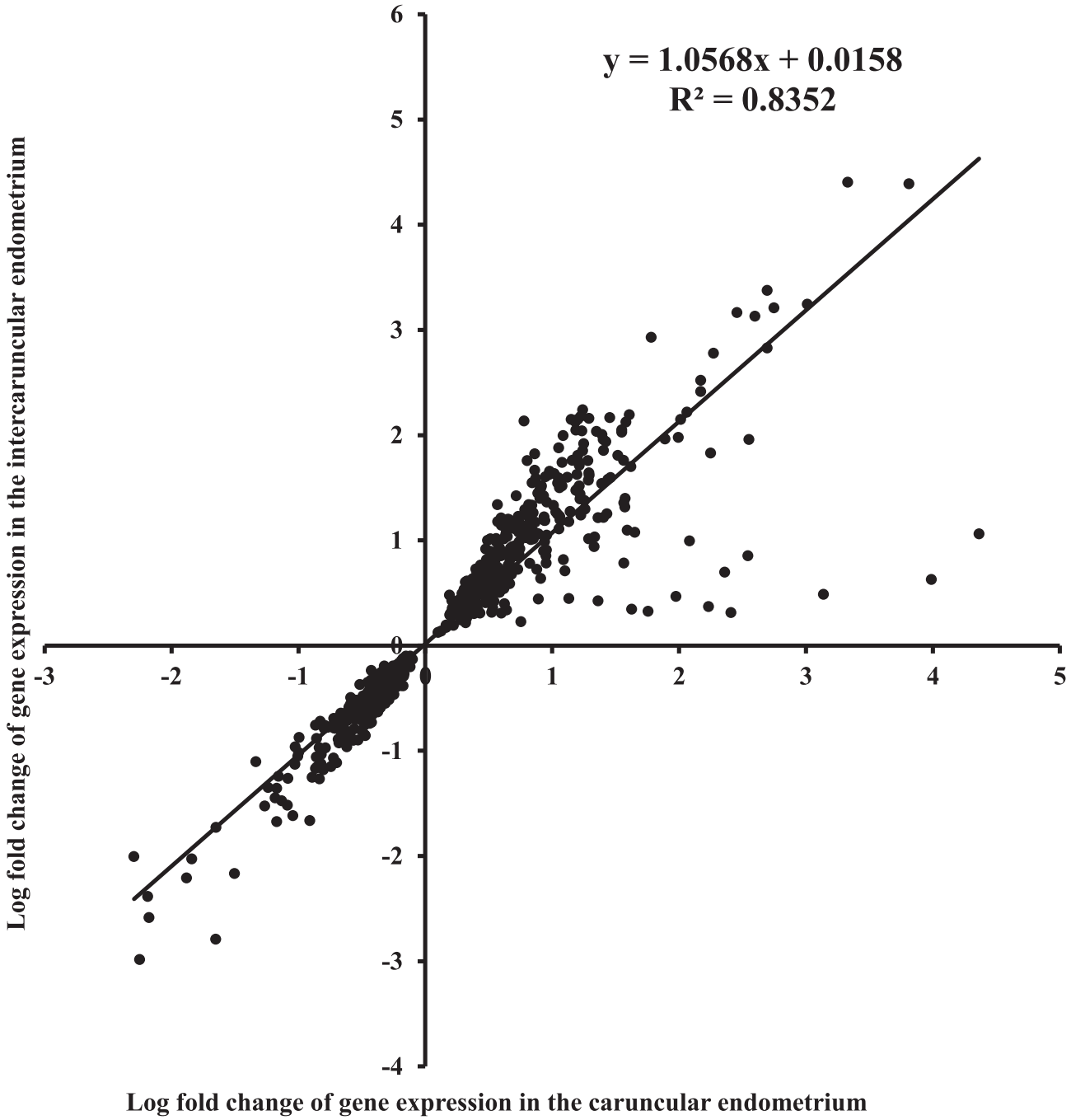

Figure 1. Linear regression of the differentially expressed genes in the intercaruncular and caruncular endometrium between days 28 to 42 of gestation.

increased conversion of acyl-coenzyme A ($P < 0.0005$, ZS = 2); increased metabolism of nucleic acid component or derivative ($P < 0.004$, ZS = 2.25); increased steroid metabolism ($P < 0.0000024$, ZS = 2.69); increased synthesis of cholesterol ($P < 0.0000013$, ZS = 2.17), lipid ($P < 0.0000001$, ZS = 2.01), steroid ($P < 0.002$, ZS = 2.41), and sterol ($P < 0.000004$, ZS = 2.16); and decreased adhesion of blood platelets ($P < 0.0007$, ZS = –2.59), and decreased apoptosis of endothelial cell lines ($P < 0.008$: ZS = –2.21) in lactating cows compared with nonlactating cows. Regulator effects analysis identified one network (Figure 2) with a consistency score of 31.231 that combined 25 potential upstream regulators (*ACACB*, *ADRB*, *AGT*, *ATP7B*, *CYP51A1*, *ELOVL5*, *INSIG1*, *INSIG2*, *INSR*, *MBTPS1*, *MGEA5*, N-cor, *NPPB*, *NR1H2*, *NR1H3*, *NR0B2*, *PEX5L*, *POR*, *PPARGC1B*, *SCAP*, *SREBF1*, *SREBF2*, Srebp, *SIRT2*, and *SIRT6*), 24 differentially expressed genes (*ACLY*, *ACSS2*, *APOA1*, *APOA4*, *CYP11A1*, *CYP2E1*, *DBI*, *DHCR7*, *FASN*, *FDFT1*, *FDPs*, *HMGCR*, *IDI1*, *LIPC*, *LSS*, *MSMO1*, *NPC1*, *NSDHL*, *PMVK*, *SCARB1*, *SCD*, *SQLE*, and *TNFRSF12A*), and three downstream effects (conversion of acyl-coenzyme A, steroid metabolism, and synthesis of sterol) with increased activity in lactating cows compared with nonlactating cows. Analysis by DAVID (Supplementary Table S15) identified upregulation of the GO terms

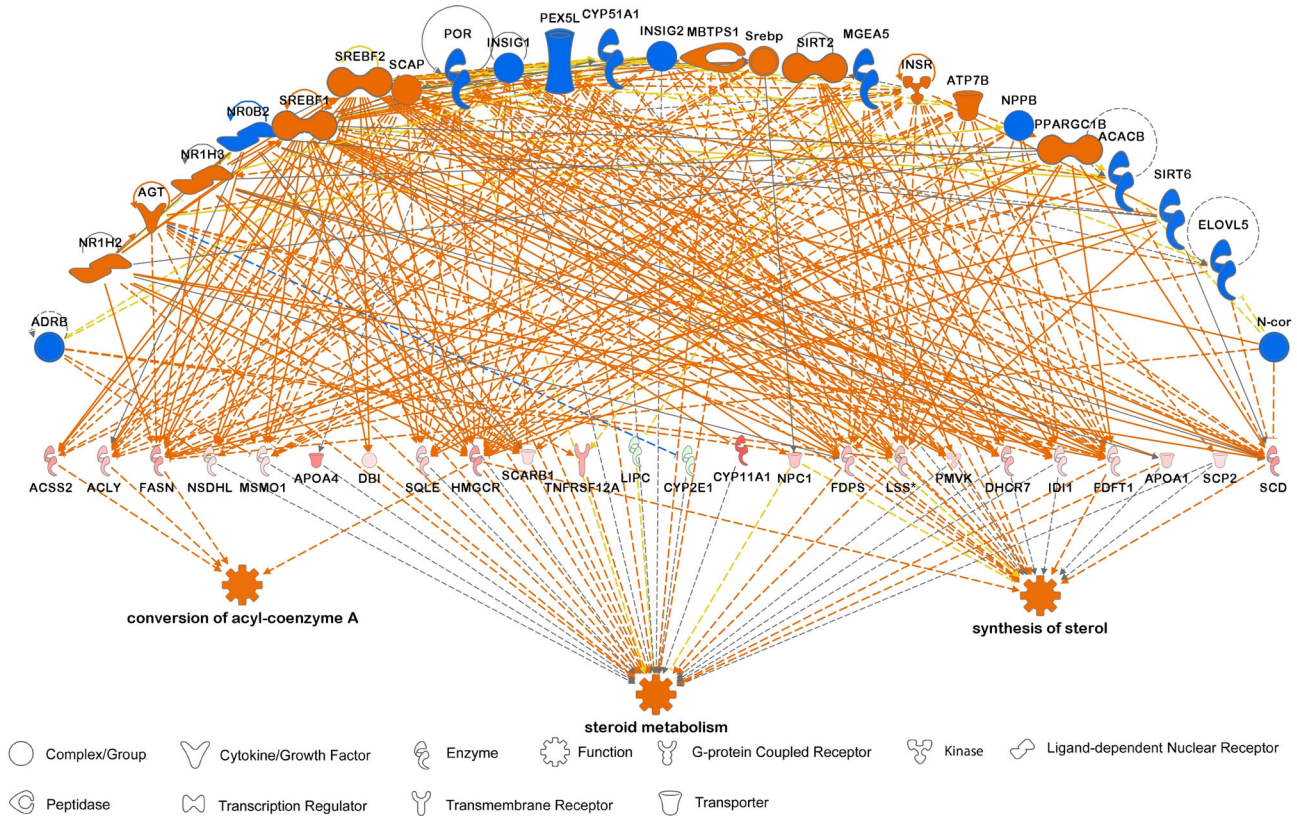

Figure 2. Network 1 generated by the regulator effect network analysis of the liver transcriptome in IPA. The network combined 25 potential upstream regulators and 24 differentially expressed genes involved in the increased conversion of acyl-coenzyme A, steroid metabolism, and synthesis of sterol in the liver of lactating cows compared with nonlactating cows. Orange and blue symbols at the top are predicted upstream and downstream regulators. Pink and green symbols represent genes up and down regulated in the lactating and nonlactating cows, respectively, with the intensity of color reflecting the degree of differential expression.

"cholesterol biosynthetic process" (BH $P < 1.3 \times 10^{-10}$), "isoprenoid biosynthetic process" (BH $P < 1.9 \times 10^{-4}$), "sterol biosynthetic process" (BH $P < 0.05$) and "oxidation-reduction process" (BH $P < 0.0008$) in lactating cows compared with nonlactating cows.

Changes in the intercaruncular endometrium transcriptome from day 28 to 42 of gestation

Of the 4516 differentially expressed transcripts (BH $P \leq 0.01$) in intercaruncular endometrium from day 28 and 42 of gestation (Supplementary Table S3), a dataset of 3022 genes (1288 upregulated and 1734 downregulated on day 42 compared with day 28) was retained for IPA. Two canonical pathways, NRF2-mediated oxidative stress response ($P = 9.99E{-}03$, ZS = 2.10) and production of nitric oxide and reactive oxygen species in macrophages ($P = 4.82E{-}02$, ZS = 2.83), had significantly greater activation on day 42 compared with day 28. Downstream effects analysis predicted the involvement of 52 specific biological functions that related to greater activation of inflammatory response, immune cell trafficking, hematological system development and function, cell-to-cell signaling and interaction, and cell movement and lesser activation of cell death and survival, and organismal injury and abnormalities on day 42 compared with day 28 (Supplementary Table S16). Briefly, the ten most significantly different biological functions were increased ingestion of cells ($P < 0.0003$, ZS = 3.1), increased pancreatic tumor ($P < 0.0005$, ZS = 2.09), decreased infection of HIV-1 ($P < 0.0007$, ZS = –3.54), increased chemotaxis of macrophage cancer cell lines ($P < 0.0009$, ZS = 2.75), increased metabolism of protein ($P < 0.002$, ZS = 3.03), increased chemotaxis of phagocytes ($P < 0.002$, ZS = 5.30), increased alternative complement pathway ($P < 0.002$, ZS = 2.43), increased phagocytosis of phagocytes ($P < 0.003$, ZS = 4.43), increased tumorigenesis of digestive organ tumor ($P < 0.003$, ZS = 2.66), and increased chemotaxis of neutrophils ($P < 0.003$, ZS = 3.83) on day 42 compared with day 28. Regulator effects analysis identified six networks. The three highest ranked networks are described. Network one with a consistency score of 9.812 combined three potential upstream regulators (*ALDH1A2*, *NCSTN*, *TXN2*), 15 differentially expressed genes (*BGN*, *CD14*, *CD44*, *CD68*, *COL1A2*, *CSF1*, *CSF1R*, *CYBA*, *CYBB*, *FCER1G*, *FCGR2B*, *NCF1*, *RAC1*, *SPARC*, *SPI1*), seven downstream effects with increased activity (engulfment of antigen presenting cells, engulfment of myeloid cells, engulfment of phagocytes, phagocytosis of leukocytes, respiratory burst, response of antigen presenting cells, response of phagocytes), and one downstream effect with decreased activity (abnormal bone density) on day 42 compared with day 28. Network two with a consistency score of 9.17 combined three potential upstream regulators (*CTSB*, Ren2, *PDGFB*), 22 differentially expressed genes (*C3*, *CCND1*, *CD44*, *CSF1*, *CSF1R*, *CXCL2*, *CYBB*, *EDN1*, *EDNRB*, *FOS*, *INHBA*, *JUN*, *LBP*, *LGALS3*, *PLAUR*, *PLCG2*, *RAC1*, *SPI1*, *SPP1*, *SYK*, *TGFB1*, *THBS1*), one downstream effect with decreased activity (high bone mass disease),

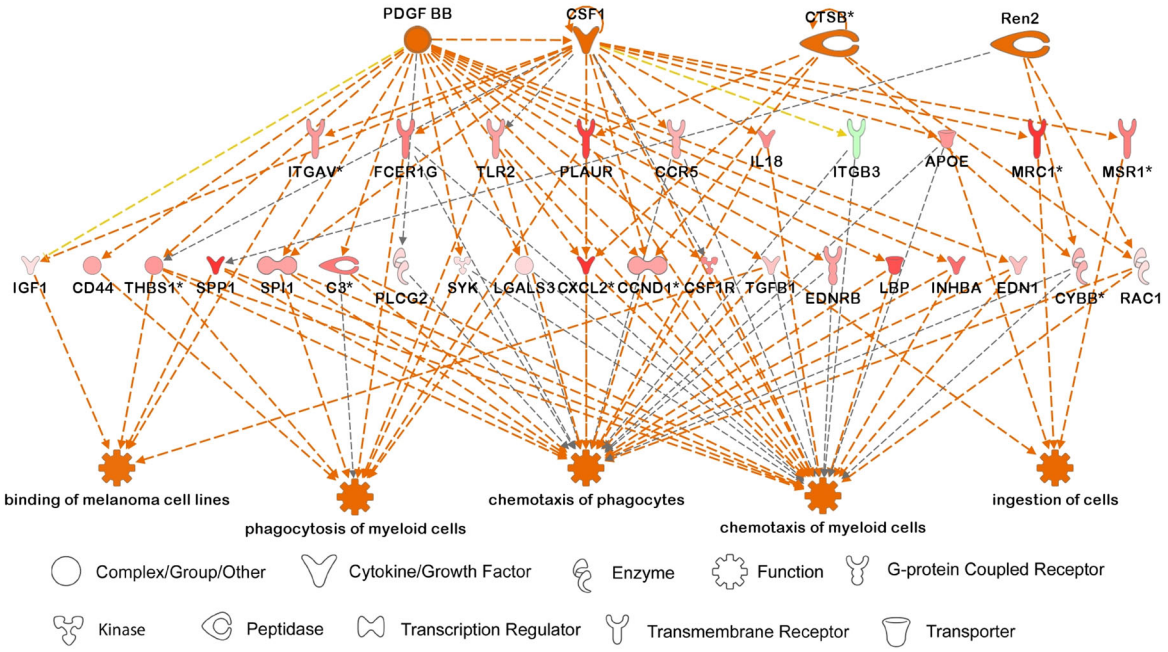

Figure 3. Network 3 generated by the regulator effect network analysis of the intercaruncular endometrium transcriptome in IPA. The network combined four potential upstream regulators and 29 differentially expressed genes involved in the increased chemotaxis of myeloid cells, chemotaxis of phagocytes, ingestion of cells, phagocytosis of myeloid cells, and binding of melanoma cell lines on day 42 compared day 28 of gestation. Orange symbols at the top are predicted upstream regulators. Pink and green symbols represent genes up- and downregulated on day 42 compared with day 28, respectively, with the intensity of color reflecting the degree of differential expression.

and three downstream effects with increased activity (chemotaxis of myeloid cells, chemotaxis of phagocytes, and phagocytosis of myeloid cells) on day 42 compared with day 28. Network three (Figure 3) with a consistency score of 7.43 combined four potential upstream regulators (*CSF1*, *CTSB*, *PDGFB*, Ren2), 29 differentially expressed genes (*APOE*, *C3*, *CCND1*, *CCR5*, *CD44*, *CSF1R*, *CXCL2*, *CYBB*, *EDN1*, *EDNRB*, *FCER1G*, *IGF1*, *IL18*, *INHBA*, *ITGAV*, *ITGB3*, *LBP*, *LGALS3*, *MRC1*, *MSR1*, *PLAUR*, *PLCG2*, *RAC1*, *SPI1*, *SPP1*, *SYK*, *TGFB1*, *THBS1*, *TLR2*), and five downstream effects with increased activity (chemotaxis of myeloid cells, chemotaxis of phagocytes, ingestion of cells, phagocytosis of myeloid cells, binding of melanoma cell lines) on day 42 compared with day 28. Analysis by DAVID (Supplementary Table S17) identified downregulation of 23 terms (generally related to transcription processes) and upregulation of eight terms including "inflammatory response" (BH $P < 0.03$), "oxidation-reduction process" (BH $P < 0.03$), "retrograde protein transport, ER to cytosol" (BH $P < 0.04$), and "positive regulation of fibroblast proliferation" (BH $P < 0.04$) on day 42 compared with day 28.

Changes in the caruncular endometrium transcriptome from day 28 to 42 of gestation

Of the 855 transcripts differentially expressed (BH $P \leq 0.01$) in caruncular endometrium from day 28 and 42 of gestation (Supplementary Table S6), a dataset of 632 genes (360 upregulated and 272 downregulated on day 42 compared with day 28) was retained for IPA. The canonical pathway, NRF2-mediated oxidative stress response ($P = 9.32E{-}03$, ZS = 2.646), was significantly activated on day 42 compared with day 28. Downstream effects analysis predicted the involvement of 17 specific biological functions that were related to increased activation of amino acid metabolism, carbohydrate metabolism, lipid metabolism, immune cell trafficking, and vascularization on day 42 compared with day 28 (Supplementary Table S18). The ten most significantly different biological functions were increased transmigration of macrophages ($P < 0.0002$, ZS = 2.0), binding of cells ($P < 0.001$, ZS = 2.98), growth of vessel ($P < 0.002$, ZS = 2.61), invasion of cells ($P < 0.002$, ZS = 2.16), conversion on basic amino acid ($P < 0.003$, ZS = 2.0), conversion of glutamine family amino acid ($P < 0.003$, ZS = 2.0), migration of bone marrow-derived macrophages ($P < 0.003$, ZS = 2.21), proliferation of epithelial cell lines ($P < 0.003$, ZS = 2.01), cell movement of myeloid cells ($P < 0.003$, ZS = 2.89), and decreased activation of thrombosis ($P < 0.003$, ZS = –2.61) on day 42 compared with day 28. Regulator effects analysis identified three networks. Network one with a consistency score of 12.41 combined two potential upstream regulators (*CSF1*, *FOXM1*), 12 differentially expressed genes (*ATF2*, *CCND1*, *CD68*, *CXCL2*, *HSP90B1*, *IL6ST*, *ITGAV*, *MRC1*, *PLAUR*, *SFRP1*, *STAB1*, *VEGFA*), seven downstream effects with increased activity (activation of antigen presenting cells, activation of phagocytes, binding of cells, cell movement of myeloid cells, migration of phagocytes, neoplasia of tumor cell lines, proliferation of epithelial cell lines) on day 42 compared with day 28. Network two with a consistency score of 5.67 combined five potential upstream regulators (*CSF1*, *CSF2*, *ERBB2*, *JUN*, let-7), seven differentially expressed genes (*BUB1B*, *CCNA2*, *CCND1*, *CTSB*, *HGF*, *MMP7*, *SDC1*), two downstream effects with increased activity (migration of bone marrow-derived macrophages and tumorigenesis of digestive organ tumor) on day 42 compared with day 28. Network three with a consistency score of 2.83 combined three potential upstream regulators (*CSF1*, *JUN*, and *TGFB1*), two differentially expressed genes

(*CCND1*, *STAB1*), and one downstream effect with increased activity (transmigration of macrophages) on day 42 compared with day 28. Analysis by DAVID (Supplementary Table S17) identified downregulation of the GO term "regulation of transcription, DNA-templated" (BH $P < 0.01$) on day 42 compared with day 28.

Differences in the endometrium transcriptome between caruncular and intercaruncular regions

Of the 5232 differentially expressed transcripts (BH $P \leq 0.01$) between caruncular and intercaruncular endometrium (Supplementary Table S11), a dataset of 3489 genes (1968 with greater expression and 1521 with reduced expression in caruncular endometrium compared with intercaruncular endometrium) was retained for IPA. Nine canonical pathways were significantly activated in caruncular endometrium compared with intercaruncular endometrium. These were PKC0 signaling in T lymphocytes ($P = 0.0002$, ZS = 3.32), NFκB signaling ($P = 0.002$, ZS = 2.78), calcium-induced T lymphocyte apoptosis ($P = 0.01$, ZS = 2.67), TREM1 signaling ($P = 0.01$, ZS = 2.24), role of NFAT in regulation of the immune response ($P = 0.01$, ZS = 3.36), production of nitric oxide and reactive oxygen species in macrophages ($P = 0.02$, ZS = 3.81), IL-8 signaling ($P = 0.02$, ZS = 2.02), SAPK/JNK signaling ($P = 0.03$, ZS = 2.19), and dendritic cell maturation ($P = 0.04$, ZS = 3.48). The canonical pathway PPAR signaling ($P = 0.03$, ZS = –2.414) was significantly inhibited in caruncular endometrium compared with intercaruncular endometrium. Downstream effects analysis predicted the involvement of 151 specific biological functions (Supplementary Table S19) that related to greater activation of hematological system development and function, lymphoid tissue structure and development, cellular development, inflammatory response, cellular movement, cellular function, immune cell trafficking, hematopoiesis, cell-to-cell signaling and interaction, and tissue morphology in caruncular endometrium compared with intercaruncular endometrium. The ten most significantly different biological functions were greater activation of cell movement ($P < 1.79 \times 10^{-26}$, ZS = 5.17), migration of cells ($P < 3.60 \times 10^{-26}$, ZS = 5.05), differentiation of cells ($P < 1.60 \times 10^{-25}$, ZS = 2.79), cellular homeostasis ($P < 1.13 \times 10^{-21}$, ZS = 2.41), quantity of blood cells ($P < 3.01 \times 10^{-21}$, ZS = 2.48), quantity of leukocytes ($P < 3.48 \times 10^{-20}$, ZS = 2.83), migration of blood cells ($P < 4.96 \times 10^{-20}$, ZS = 4.649), leukocyte migration ($P < 7.36 \times 10^{-20}$, ZS = 4.61), immune response of cells ($P < 3.49 \times 10^{-19}$, ZS = 2.53), and differentiation of blood cells ($P < 4.77 \times 10^{-19}$, ZS = 4.54) in caruncular endometrium compared with intercaruncular endometrium. Regulator effects analysis identified 17 networks and the three highest ranked networks are summarized here. Network one with a consistency score of 28.622 combined one potential upstream regulator (integrinα), five differentially expressed genes (*ITGAM*, *ITGAL*, *ITGB2*, *TLR2*, *TLR4*), 17 downstream effects with greater activity in caruncular endometrium compared with intercaruncular endometrium (activation of leukocytes; adhesion of granulocytes and phagocytes; arthritis; binding of blood cells; cell movement of leukocytes; cell viability of leukocytes; cellular infiltration of cells; development of lymphocytes; differentiation of leukocytes; engulfment of cells; hypersensitive reaction; phagocytosis; quantity of CD4+ T-lymphocytes; recruitment of phagocytes; T cell homeostasis; and transmigration of blood cells). Network two with a consistency score of 6.197 combined four potential upstream regulators (*CSF1*, *FN1*, *ITGAV*, and *ITGB6*), 15 differentially expressed genes (*CCL4*, *CCL5*, *CCR5*, *CXCL2*, *CXCL5*, *CXCL8*, *IL1A*, *IL1R1*, *ITGAM*, *MMP2*, *SERPINE1*, *SFRP1*, *TLR2*), and two downstream effects with greater activity (recruitment of neutrophils and trafficking of macrophages) in caruncular endometrium compared with intercaruncular endometrium. Network three with a consistency score of 5.965 combined three potential upstream regulators (*FN1*, *ITGAV*, *ITGB6*), 19 differentially expressed genes (*CCL2*, *CCL4*, *CCL5*, *CDH1*, *COL1A1*, *COL1A2*, *CXCL2*, *CXCL5*, *CXCL8*, *GPX1*, *IL1R1*, *ITGAM*, *ITGB3*, *MMP2*, *NFKBIA*, *SERPINE1*, *TGFB1*, *TGFBR2*, *TP53*), two downstream effects with reduced activity (enteritis, inflammation of intestine), and one downstream effect with increased activity (recruitment of granulocytes) in caruncular endometrium compared with intercaruncular endometrium.

Changes in the placenta transcriptome from day 28 to 42 of gestation

Of the 2396 differentially expressed transcripts (BH $P \leq 0.01$) in the placenta between day 28 and 42 of gestation (Supplementary Table S8), a dataset of 1600 genes (629 upregulated and 971 downregulated on day 42) was retained for IPA. The canonical pathway, EIF2 signaling ($P = 4.69E{-}06$, ZS = –4.24), was significantly inhibited on day 42 compared with day 28. Downstream effects analysis (Supplementary Table S20) predicted increased activation cell death of osteosarcoma cells ($P < 0.002$, ZS = 4.04), increased activation of mitosis of cervical cancer cell lines ($P < 0.002$, ZS = 2.24), increased activation of migration of antigen presenting cells (0.009; ZS = 2.06), increased activation of expression of RNA ($P < 0.01$, ZS = 3.47), increase activation of migration of macrophages ($P < 0.01$; ZS = 2.46), decreased activation of lysosomal storage disease ($P < 0.004$; ZS = -2.21), decreased activation of cytokinesis of tumor cell lines ($P < 0.006$; ZS = –2.18), decreased activation of infection of lymphocytic choriomeningitis virus ($P < 0.007$; ZS = –2.0), and decreased activation of transport of phospholipid ($P < 0.01$, ZS = –2.18) on day 42 compared with day 28. Regulator effects analysis identified five networks. The three highest ranked are described. Network 1 with a consistency score of 7.82 combined 11 potential upstream regulators (*APOE*, *CDKN2A*, Hdac, Jnk, *MAP2K1*, *MAPK8*, *MYD88*, *P38 MAPK*, *PDGFB*, *RBL2*, *TLR3*), 20 differentially expressed genes (*ASAH1*, *AURKB*, *BIRC5*, *CCL2*, *CD14*, *CSF1R*, *CTSD*, *CXCL10*, *CXCR4*, *CYBB*, *GUSB*, *KIFC1*, *LIPA*, *LRP1*, *NEK2*, *NOS2*, *NPM1*, *SERPINE1*, *SPP1*, *WNT5A*), one downstream effect with increased activity (migration of macrophages), and two downstream effects with reduced activity (lysosomal storage disease and cytokinesis of tumor cell lines) on day 42 compared with day 28. Network 2 with a consistency score of 7.11 combined four potential upstream regulators (*MYC*, *MYCN*, *RICTOR*, *XBP1*), 19 differentially expressed genes (*COPB2*, *COPG1*, *COPZ1*, *CXCL10*, *EIF3G*, *RPL13*, *RPL19*, *RPL27*, *RPL27A*, *RPL3*, *RPL38*, *RPL7*, *RPL7A*, *RPLP0*, *RPS18*, *RPS21*, *RPS3*, *RPS7*, *RRM2*), one downstream effect with increased activity (cell death of osteosarcoma cells), and downstream effect with reduced activity (infection by lymphocytic choriomeningitis virus) on day 42 compared with day 28. Network 3 with a consistency score of 2.04 combined one potential upstream regulator (*AREG*), six differentially expressed genes (*CXCR4*, *EGFR*, *ELK1*, *FOS*, *HAS2*, *JUN*), and one downstream effect with increased activity (invasion of cells) on day 42 compared with day 28. Analysis by DAVID (Supplementary Table S16) identified downregulation of GO terms "tricarboxylic acid" (BH $P < 0.01$), the "oxidation-reduction" process (BH $P < 0.0004$), and six GO terms related to

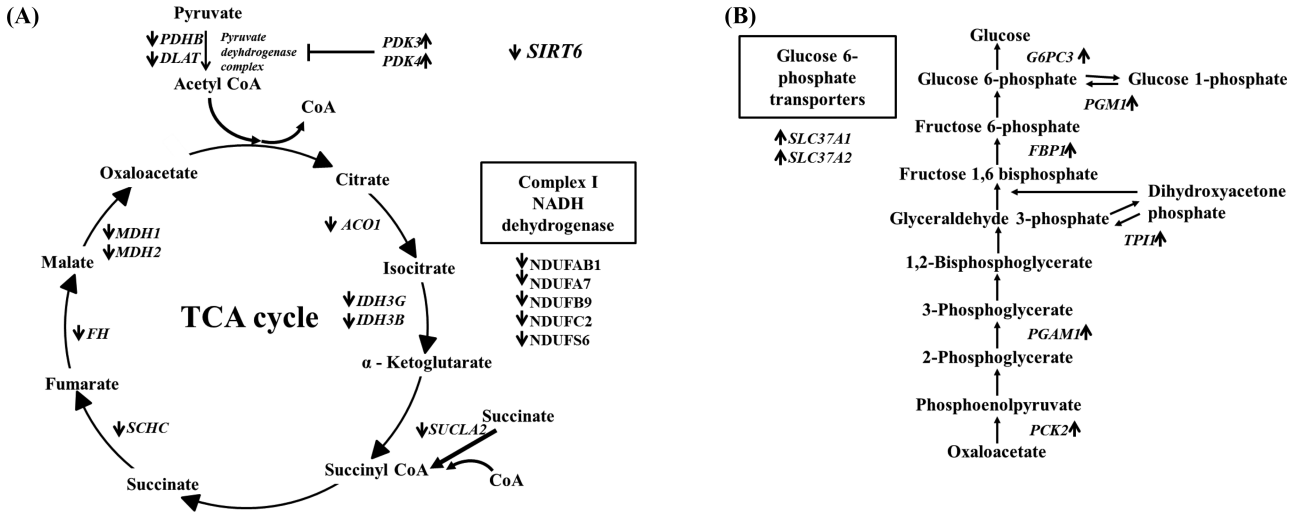

Figure 4. Glucose metabolism in the endometrium and placenta. Transcriptome analysis supported downregulation of the TCA cycle in the placenta from day 28 to 42 of gestation (A), and upregulation of gluconeogenesis in the intercaruncular endometrium (B).

translation (BH $P < 7.5 \times 10^{-13}$–0.03) and upregulation of the GO term "positive regulation of transcription from RNA polymerase II promoter" (BH $P < 5.7 \times 10^{-9}$) on day 42 compared with day 28.

Discussion

Contrary to our hypothesis, the transcriptomes of the caruncular endometrium, intercaruncular endometrium and placenta in postpartum Holstein cows were not significantly affected by lactation. This was surprising considering that placental weight and fetal weight were approximately 50% and 25% greater in the nonlactating cows compared with the lactating cows [9]. Dynamic changes in the transcriptome of the bovine endometrium and placenta were identified, however, that coincided with the establishment and development of the placenta, and the completion of conceptus attachment to the endometrium. These transcriptome changes were temporally, but not linearly regulated, with the greatest differences observed between day 42 vs. 28 of gestation; followed by day 35 vs. 28 of gestation; with only minor differences between day 42 vs. 35 of gestation. The transcriptome changes were also tissue-specific; with the temporal response consistently greatest in the intercaruncular endometrium, followed by the placenta, and caruncular endometrium.

Glucose is the principal source of energy for the developing pregnancy [23] and changes in substrate availability would be, therefore, an important determinant of conceptus growth rate during this window of development. In previous work, we reported that nonlactating cows had greater placental fluid and circulating concentrations of glucose and fructose [11]. One possible explanation for our observations is that the extreme metabolic differences created by the lactating/nonlactating cow model altered substrate availability to the conceptus while not affecting the gene expression pattern within the tissues themselves. There was, however, a significant downregulation of the TCA cycle in the placenta by day 42 (Figure 4a). Components of the pyruvate dehydrogenase complex (*PDHB* and *DLAT*) were also downregulated and kinases that inactivate pyruvate dehydrogenase (*PDK3* and *PDK4*) were upregulated (Figure 4b). This shift in glucose metabolism is evidence for the establishment of aerobic glycolysis or the "Warburg Effect" in placenta from day 28 to 42 of gestation where pyruvate is not fully oxidized but instead is used to generate lactate [24]. The downregulation of *SIRT6* in the placenta may enable the shift to aerobic glycolysis that was observed [25]. Greater mRNA abundance of the rate-limiting gluconeogenic genes (*FBP1*, *PCK2*, and *G6PC3*) in the intercaruncular endometrium was also detected (Figure 4b), indicating that the uterus itself had become a gluconeogenic organ by day 42 perhaps in an effort to supply glucose to the developing pregnancy. A recent study from our laboratory reported that growth of the pregnancy was independent of the cow's own metabolic status; i.e., circulating concentrations of glucose, fatty acids, insulin, and insulin-like growth factor 1 [26]. It is likely, however, that the extremes of glucose in the current lactating/nonlactating cow model were greater than that typically found in a population of dairy cows.

It should be noted that this study only collected tissue from cows with an established 28 to 42 day pregnancy. Despite similar transcriptome profiles between lactating and nonlactating cows in the current study, data from other similar studies would suggest that the differences in pregnancy development were manifested earlier in the reproductive cycle. Lactating and nonlactating cows have unique follicular fluid fatty acid and amino acid profiles [27] that may affect oocyte competence. Blastocyst development was greater in nonlactating cows compared with lactating cows [28] and lactation status did affect the endometrial transcriptome during maternal recognition of pregnancy [13]. There is, however, disagreement, on the association between dairy cow milk production and fertility, with the literature ranging from negative [29], neutral [30], to positive [31,32]. Recent discussion has deemed this hypothesis simplistic, with large variation within and between herds [33]. Instead, the occurrence of uterine and systemic inflammation, the rapid depletion of adipose reserves, and the delayed resumption of ovarian cyclicity postpartum are now deemed more appropriate risk factors for subsequently compromised fertility in the lactating dairy cow [32,34–37].

Analysis of the liver transcriptome from day 28 to 42 of gestation (81–176 days in milk) was included in the study to act as a positive control for the effects of lactation on tissue gene expression. By using liver tissues collected from the same cows and at the same time as reproductive tissues, we attempted to address a potential criticism that lactation had minimal effect on any tissue within the

cow. This was clearly not the case as the liver transcriptome was vastly different between the lactating and nonlactating cows with 715 differentially expressed genes. More importantly, the expression profile highlighted differences in key biological functions that would have been expected. For example, greater conversion of acyl-coenzyme A, synthesis of cholesterol, and steroid metabolism in the lactating cows compared with the nonlactating cows would support the current knowledge of the adaptations in liver lipid metabolism during the postpartum period [38–42]. These results also represent the most likely mechanism explaining greater circulating concentrations of fatty acids in lactating cows compared with nonlactating cows [9,10].

The majority of genes differentially expressed from day 28 to 42 of gestation in caruncular endometrium were also differentially expressed (85%) in the intercaruncular endometrium. All of the 727 genes in common had a similar expression pattern, and were highly correlated. The common features of differential gene expression across the two tissue types may in part be explained by common cell types as well as some cross-contamination of caruncular endometrium with adjacent intercaruncular endometrium during tissue collection.

Some of the most highly differentially expressed genes have well-described roles in bovine reproductive biology. The IGF system, for example, is known to be involved in bovine reproduction [43,20,44,32] and components of the IGF system were detected in the endometrium and placenta. The mRNA abundance of *IGF1*, *IGF2R*, *IGFBP2*, *IGFBP4*, and *IGFBP6* were increased from day 28 to 42 in the intercaruncular endometrium; *IGF2R* and *IGFBP2* were increased from day 28 to 42 in the caruncular endometrium; and *IGF2* and *IGFBP3* were increased from day 28 to 42 in the placenta. In intercaruncular endometrium, a pronounced downregulation of interferon-stimulated genes was evident, with *ISG15*, *OAS1*, and *MX1* being the 5th, 10th, and 41th-most downregulated genes. Similarly, *TKDP4*, a known product of early pregnancy [45] was the 14th-most downregulated gene. The observation that these genes are highly downregulated illustrates an important element of the data presented. Genes with that are highly expressed early in pregnancy (for example those responding to interferon-τ) will appear as downregulated by day 42 of gestation. Other genes likely to be of importance included *PRLR*, *ANXA10*, and *LOC512548* (three most upregulated genes from day 28 to 42 of gestation) and *TDGF1*, *PIP*, *BPIFB1* (three most downregulated genes from day 28 to 42 of gestation) that were differentially expressed in both the caruncular and intercaruncular endometrium. The function of some of these genes with respect to the early pregnant uterus is incompletely understood. Additionally, the pregnancy-associated glycoproteins, *PAG17*, *PAG1*, and *PAG9*, were the 3rd, 7th, and 22nd most differentially expressed genes (all upregulated from day 28 to 42 of gestation) in the caruncular endometrium. This observation could be explained by the invasion of the cotyledonary tissue into the caruncles. Our manual separation procedure could not have removed this form of contamination.

It is well recognized that pregnancy development involves morphological changes that affect the composition of the tissues collected. This was particularly true of the placenta where the day 28 placenta had poorly developed cotyledons whereas by day 42 the cotyledonary tissue was well developed and attached to the maternal caruncle. In all likelihood, a day 42 sample had a greater percentage of cotyledonary tissue, but we did not attempt to measure this percentage or separate tissue types prior to RNA extraction. It was also true that a day 42 caruncle would be partially contaminated with placental tissue arising from the cotyledon.

The recruitment of macrophages to the endometrium during pregnancy is one of the major immune responses to pregnancy [46–48]. The current study supports this observation and also indicates macrophage recruitment to the placenta. In addition to macrophage recruitment featuring prominently in the IPA results, the mRNA abundance of the macrophage-specific markers *CD14* and *CD68* increased in both regions of the endometrium and in the placenta on day 42 compared with day 28. Greater activation of the alternative complement pathway, based on greater expression of *C1QA*, *C3*, *CD55*, *CFB*, *CFD*, and *CFP* by day 42, provides further evidence of an increased inflammatory response in the intercaruncular endometrium during this period. The exact role of macrophages during pregnancy development and the signal(s) for their recruitment remain unknown, but the removal of apoptotic cells or the secretion of growth factors may be important [46,49,50]. Macrophages have been classified as either pro-inflammatory (M1) or anti-inflammatory (M2) based on their activation to either produce nitric oxide and reactive oxygen species or to increase arginine metabolism to ornithine, respectively [51]. Genes that differentiate between M1 and M2 were differentially expressed between day 28 and 42 of gestation [52,53] indicating that both populations of macrophages were present. Interestingly, the pathways "production of nitric oxide and reactive oxygen species in macrophages," and "NRF2-mediated oxidative stress response" were more activated by day 42 in the intercaruncular endometrium, and in the intercaruncular and caruncular endometrium, respectively. Greater production of nitric oxide by macrophages, therefore, represents a bias towards a M1 pro-inflammatory response during this period. Both nitric oxide [54] and reactive oxygen species [55] also have angiogenic properties to promote vascular development and blood supply as the pregnancy develops. At the same time, greater activation of the NRF2-mediated oxidative stress response pathway acts to prevent cellular damage from excess reactive oxygen species [56]. The aforementioned increase in gluconeogenesis would have contributed to the metabolic requirements of the macrophages, and the shift to aerobic glycolysis in the placenta would further suggest greater activation of M1 macrophages by day 42 [57]. It has been suggested that glycolysis is more suitable than fatty acid oxidation in M1 macrophages because of the rapid, short-term bursts of activation that are required at sites of inflammation [56].

Regulator effects analysis suggested that the recruitment and phagocytic activity of myeloid cells, including macrophages by day 42 was promoted by the greater mRNA abundance of *NCSTN*, *CTSB*, *PDGFB*, and *CSF1* in the intercaruncular endometrium and by greater mRNA abundance of *CSF1* and *TGFB1* in the caruncular endometrium. In the placenta, *APOE*, a lipoprotein; *Hdac*, a histone deacetylase; and *TLR3*, a receptor involved in pathogen recognition and innate immunity activation were predicted to be upstream regulators of macrophage migration, and their expression profile supported this observation [58–60]. The involvement of *CTSB* in pregnancy development is supported by the greater intercaruncular endometrium expression of other cathepsin family members (*CTSA*, *CTSC*, *CTSD*, *CTSH*, *CTSK*, *CTSV*, and *CTSZ*) that have been implicated in the regulation of MHC class II-dependent antigen presentation and in tissue remodeling during the attachment period of pregnancy in the sheep and pig [61–63]. Greater expression of the PDGF α-receptor (*PDGFRA*) also by day 42 would support the involvement of *PDGFB* in chemotaxis and tissue remodeling during this stage of pregnancy development [64]. Greater expression of both *CSF1* and *CSF1* receptor suggests the involvement of *CSF1* receptor signaling as a mechanism for recruitment of macrophages to the

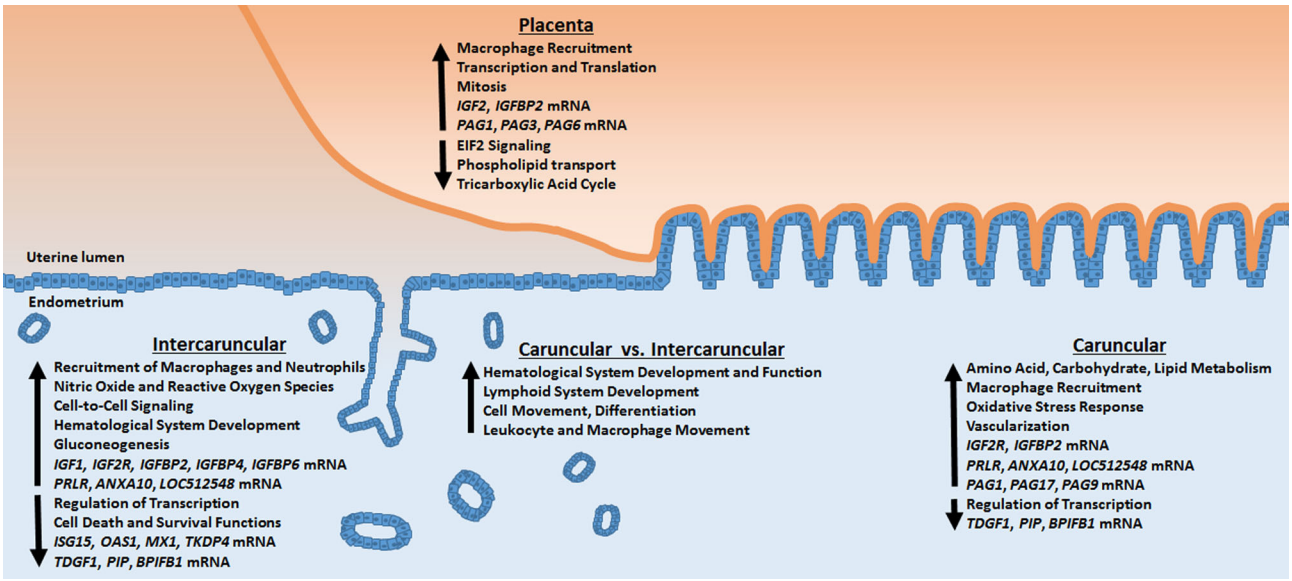

Figure 5. Schematic summary of the main biological processes regulated from day 28 to 42 of gestation in the bovine endometrium and placenta, and the main biological processes distinguishing the caruncular endometrium from the intercaruncular endometrium.

endometrium, and greater rates of tissue remodeling and angiogenesis [46,65,66].

A large difference in the transcriptome between the intercaruncular and caruncular areas was expected based on the well-established morphological and functional differences between the two regions [67–69]. Interestingly, the number of differentially expressed genes identified in the current study that coincided with the completion of attachment (5232 genes) was much greater than that reported at the onset of attachment on day 20 of pregnancy (453 genes) by Mansouri-Attia et al. (2009) [67]. It is clear that the overwhelming difference between the intercaruncular and caruncular endometrium related to the immune system. It was indicative of an amplified immune response in the caruncular endometrium, in agreement with Mansouri-Attia et al. (2009) [67] and reflective of a more intense immune response at the feto–maternal interface. This was represented by an expression profile that suggested greater recruitment, differentiation, survival, and activity of both myeloid and lymphoid immune cells in the caruncular endometrium. Integrins are a family of transmembrane glycoproteins that reorganize extracellular matrix and cytoskeleton into aggregates at the adhesion sites [70] and were predicted to be upstream regulators of the recruitment, differentiation, survival, and activity of both myeloid and lymphoid immune cells to the caruncular endometrium. Although only *ITGAV* was differentially expressed between the caruncular and intercaruncular endometrium (greater mRNA abundance in the intercaruncular endometrium), other integrins may be present at the protein level and be involved in the attachment of the cotyledons and caruncles [71,72]. Differences between the two regions included also greater activation of processes related to hematological and lymph system development, and tissue morphology in the caruncular endometrium. Increased vascular development, and carbohydrate, lipid, and amino acid metabolism from day 28 to 42 were primarily restricted to the caruncular endometrium and likely supported attachment with the cotyledons, and the movement of nutrients between the dam and the fetus, to support the growth of the fetus, placentome, and endometrium tissue [23,73]. Overall, these observations suggest a shift in the primary site of metabolic activity, from the intercaruncular endometrium prior to attachment to the caruncular endometrium during and after attachment [67]. They also represented a shift in importance as the pregnancy transitioned from histotrophic to placental nutrition.

There were two somewhat paradoxical trends identified in the endometrium and placenta. Both IPA and DAVID indicated decreased activation of biological processes related to transcription in the intercaruncular and caruncular endometrium. Conversely, by day 42 in the placenta, processes related to transcription were increased; yet, the EIF2 signaling pathway that initiates protein synthesis was inhibited. In the placenta, *RICTOR*, a subunit of MTORC2; *XBP1*, a transcription factor of MHC class II genes; and *MYC*, a DNA binding transcription factor were predicted to be upstream regulators of cell death, and their expression profile (*RICTOR* increased; *MYC* and *XBP1* decreased) suggested that cell survival processes were increased by day 42. This role of these transcription- and translation-related observations is unknown.

The current study reinforced previous observations that the transcriptome of the uterus and conceptus is relatively independent of the dams own metabolic environment [13,74]. The extremes in circulating and uterine glucose between the lactating and nonlactating cows offer the most likely explanation for the differences in pregnancy development, although effects of the ovary, oviduct, and uterine environment earlier during pregnancy development cannot be ruled out. This study provides a comprehensive landscape of transcriptome developments in the bovine endometrium and placenta from day 28 to 42 of gestation (summarized in Figure 5); and serves as a resource for future studies on the biological mechanisms associated with bovine pregnancy development and/or pregnancy loss.

Supplementary data

Supplementary data are available at *BIOLRE* online.

Supplementary Figure S1a-d. Principal component analysis of all tissues (1a), and of the liver (1b), endometrium (1c), and placenta (1d).

Supplementary Table S1. Gene name, GenBank number, oligonucleotide primer sequence (forward and reverse primers; 5′ to 3′), location of the primer within the GenBank sequence, length of the amplicon (bp), and amplification efficiency for the individual genes whose expression was measured by reverse transcription polymerase chain reaction (RT-PCR).
Supplementary Table S2. Liver genes differentially expressed between lactating and nonlactating cows.
Supplementary Table S3. Intercaruncular endometrium genes differentially expressed between day 28 and 42 of gestation.
Supplementary Table S4. Intercaruncular endometrium genes differentially expressed between day 28 and 35 of gestation.
Supplementary Table S5. Intercaruncular endometrium genes differentially expressed between day 35 and 42 of gestation.
Supplementary Table S6. Caruncular endometrium genes differentially expressed between day 28 and 42 of gestation.
Supplementary Table S7. Caruncular endometrium genes differentially expressed between day 28 and 35 of gestation.
Supplementary Table S8. Placenta genes differentially expressed between day 28 and 42 of gestation.
Supplementary Table S9. Placenta genes differentially expressed between day 28 and 35 of gestation.
Supplementary Table S10. Placenta genes differentially expressed between day 42 and 35 of gestation.
Supplementary Table S11. Genes differentially expressed between caruncular and intercaruncular endometrium.
Supplementary Table S12. Relative mRNA expression for selected genes within intercaruncular endometrium, caruncular endometrium, and placenta that were identified as differentially expressed for 42 vs. 28 days of pregnancy in the microarray analysis and subsequently analysed by RT-PCR. For RTPCR, the data are least square means ± SEM.
Supplementary Table S13. Relative mRNA expression for selected genes within liver that were identified as differentially expressed for lactating vs. nonlactating in the microarray analysis and subsequently analysed by RT-PCR. For RTPCR, the data are least square means ± SEM.
Supplementary Table S14. Biological function identified by Ingenuity Pathway Analysis to be significantly activated in liver between lactating and nonlactating cows.
Supplementary Table S15. Gene ontology analysis of differentially expressed genes in the liver between lactating and nonlactating cows.
Supplementary Table S16. Biological functions identified by Ingenuity Pathway Analysis to be significantly activated in intercaruncular endometrium from day 28 to 42 of gestation.
Supplementary Table S17. Gene ontology analysis of differentially expressed genes in the intercaruncular endometrium, caruncular endometrium, and placenta from day 28 to 42 of gestation.
Supplementary Table S18. Biological functions identified by Ingenuity Pathway Analysis to be significantly activated in caruncular endometrium from day 28 to 42 of gestation.
Supplementary Table S19. Biological functions identified by Ingenuity Pathway Analysis to be significantly activated in caruncular endometrium relative to the intercaruncular endometrium
Supplementary Table S20. Biological functions identified by Ingenuity Pathway Analysis to be significantly activated in placenta from day 28 to 42 of gestation.

Acknowledgments

The authors would like to thank members of the Division of Animal Sciences at the University of Missouri including J.P. Meyer, A.M. Williams, A. Perretta, A. Brauch, C. Okamura, J. Denbigh, E. Adkins, and R. Disselhorst.

References

1. Pryce JE, Woolaston R, Berry DP, Wall E, Winters M, Butler R, Shaffer M. World trends in dairy cow fertility. In: 10th World Congress on Genetics Applied to Livestock Production, August 17–22, 2014, Vancouver, British Columbia. 2014: Article 154.
2. Wiltbank MC, Baez GM, Garcia-Guerra A, Toledo MZ, Monteiro PLJ, Melo LF, Ochoa JC, Santos JEP, Sartori R. Pivotal periods for pregnancy loss during the first trimester of gestation in lactating dairy cows. *Theriogenology* 2016; **86**:239–253.
3. Diskin M, Morris D. Embryonic and early foetal losses in cattle and other ruminants. *Reprod Domest Anim* 2008; **43**:260–267.
4. Shalloo L, Cromie A, McHugh N. Effect of fertility on the economics of pasture-based dairy systems. *Animal* 2014; **8**:222–231.
5. Cabrera VE. Economics of fertility in high-yielding dairy cows on confined TMR systems. *Animal* 2014; **8**:211–221.
6. Bauman DE, Currie WB. Partitioning of nutrients during pregnancy and lactation: a review of mechanisms involving homeostasis and homeorhesis. *J Dairy Sci* 1980; **63**:1514–1529.
7. Walsh SW, Williams EJ, Evans ACO. A review of the causes of poor fertility in high milk producing dairy cows. *Anim Reprod Sci* 2011; **123**:127–138.
8. Lucy MC. Reproductive loss in high-producing dairy cattle: where will it end? *J Dairy Sci* 2001; **84**:1277–1293.
9. Green JC, Meyer JP, Williams AM, Newsom EM, Keisler DH, Lucy MC. Pregnancy development from day 28 to 42 of gestation in postpartum Holstein cows that were either milked (lactating) or not milked (not lactating) after calving. *Reproduction* 2012; **143**:699–711.
10. Thompson IM, Cerri RLA, Kim IH, Ealy AD, Hansen PJ, Staples CR, Thatcher WW. Effects of lactation and pregnancy on metabolic and hormonal responses and expression of selected conceptus and endometrial genes of Holstein dairy cattle. *J Dairy Sci* 2012; **95**:5645–5656.
11. Lucy MC, Green JC, Meyer JP, Williams AM, Newsom EM, Keisler DH. Short communication: glucose and fructose concentrations and expression of glucose transporters in 4- to 6-week pregnancies collected from Holstein cows that were either lactating or not lactating. *J Dairy Sci* 2012; **95**:5095–5101.
12. Scully S, Maillo V, Duffy P, Kelly A, Crowe M, Rizos D, Lonergan P. The effect of lactation on post-partum uterine involution in holstein dairy cows. *Reprod Domest Anim* 2013; **48**:888–892.
13. Cerri RLA, Thompson IM, Kim IH, Ealy AD, Hansen PJ, Staples CR, Li JL, Santos JEP, Thatcher WW. Effects of lactation and pregnancy on gene expression of endometrium of Holstein cows at day 17 of the estrous cycle or pregnancy. *J Dairy Sci* 2012; **95**:5657–5675.
14. Green JC, Volkmann DH, Poock SE, McGrath MF, Ehrhardt M, Moseley AE, Lucy MC. Technical note: a rapid enzyme-linked immunosorbent assay blood test for pregnancy in dairy and beef cattle. *J Dairy Sci* 2009; **92**:3819–3824.
15. Ritchie ME, Phipson B, Wu D, Hu Y, Law CW, Shi W, Smyth GK. limma powers differential expression analyses for RNA-sequencing and microarray studies. *Nucleic Acids Res* 2015; **43**:e47–e47.
16. R Development Core Team. *R: A Language and Environment for Statistical Computing*. 2008.
17. Wu J, Irizarry R, MacDonald J, Gentry J. *gcrma: Background Adjustment Using Sequence Information. R package version 2.46.0*. 2016.
18. Kauffmann A, Gentleman R, Huber W. arrayQualityMetrics–a bioconductor package for quality assessment of microarray data. *Bioinformatics* 2009; **25**:415–416.
19. Benjamini Y, Hochberg Y. Controlling the false discovery rate: a practical and powerful approach to multiple testing. *J R Stat Soc Ser B* 1995; **57**:289–300.

20. Rhoads ML, Meyer JP, Lamberson WR, Keisler DH, Lucy MC. Uterine and hepatic gene expression in relation to days postpartum, estrus, and pregnancy in postpartum dairy cows. *J Dairy Sci* 2008; **91**: 140–150.
21. Huang DW, Sherman BT, Lempicki RA. Systematic and integrative analysis of large gene lists using DAVID bioinformatics resources. *Nat Protoc* 2008; **4**:44–57.
22. Huang DW, Sherman BT, Lempicki RA. Bioinformatics enrichment tools: paths toward the comprehensive functional analysis of large gene lists. *Nucleic Acids Res* 2009; **37**:1–13.
23. Battaglia FC, Meschia G. Principal substrates of fetal metabolism. *Physiol Rev* 1978; **58**:499–527.
24. Vander Heiden MG, Cantley LC, Thompson CB. Understanding the Warburg effect: the metabolic requirements of cell proliferation. *Science* 2009; **324**:1029–1033.
25. Sebastián C, Zwaans BMM, Silberman DM, Gymrek M, Goren A, Zhong L, Ram O, Truelove J, Guimaraes AR, Toiber D, Cosentino C, Greenson JK et al. The histone deacetylase SIRT6 is a tumor suppressor that controls cancer metabolism. *Cell* 2012; **151**:1185–1199.
26. Stratman TJ, Moore SG, Lamberson WR, Keisler DH, Poock SE, Lucy MC. Growth of the conceptus from day 33 to 45 of pregnancy is minimally associated with concurrent hormonal or metabolic status in postpartum dairy cows. *Anim Reprod Sci* 2016; **168**:10–18.
27. Forde N, O'Gorman A, Whelan H, Duffy P, O'Hara L, Kelly AK, Havlicek V, Besenfelder U, Brennan L, Lonergan P. Lactation-induced changes in metabolic status and follicular-fluid metabolomic profile in postpartum dairy cows. *Reprod Fertil Dev* 2015; **28**:1882–1892.
28. Maillo V, Rizos D, Besenfelder U, Havlicek V, Kelly AK, Garrett M, Lonergan P. Influence of lactation on metabolic characteristics and embryo development in postpartum Holstein dairy cows. *J Dairy Sci* 2012; **95**:3865–3876.
29. Nebel NL, McGilliard ML. Interactions of high milk yield and reproductive performance in dairy cows. *J Dairy Sci* 1993; **76**:3257–3268.
30. Patton J, Kenny DA, McNamara S, Mee JF, O'mara FP, Diskin MG, Murphy JJ. Relationships among milk production, energy balance, plasma analytes, and reproduction in Holstein-Friesian cows. *J Dairy Sci* 2007; **90**:649–658.
31. Buckley F, O'Sullivan K, Mee JF, Evans RD, Dillon P. Relationships among milk yield, body condition, cow weight, and reproduction in spring-calved holstein-friesians. *J Dairy Sci* 2003; **86**:2308–2319.
32. Cummins SB, Lonergan P, Evans ACO, Berry DP, Evans RD, Butler ST. Genetic merit for fertility traits in Holstein cows: I. Production characteristics and reproductive efficiency in a pasture-based system. *J Dairy Sci* 2012; **95**:1310–1322.
33. Bello NM, Stevenson JS, Tempelman RJ. Invited review: milk production and reproductive performance: modern interdisciplinary insights into an enduring axiom. *J Dairy Sci* 2012; **95**:5461–5475.
34. Santos JEP, Rutigliano HM, Filho MFS. Risk factors for resumption of postpartum estrous cycles and embryonic survival in lactating dairy cows. *Anim Reprod Sci* 2009; **110**:207–221.
35. Ribeiro ES, Lima FS, Greco LF, Bisinotto RS, Monteiro APA, Favoreto M, Ayres H, Marsola RS, Martinez N, Thatcher WW, Santos JEP. Prevalence of periparturient diseases and effects on fertility of seasonally calving grazing dairy cows supplemented with concentrates. *J Dairy Sci* 2013; **96**:5682–5697.
36. Ribeiro ES, Gomes G, Greco LF, Cerri RLA, Vieira-Neto A, Monteiro PLJ, Lima FS, Bisinotto RS, Thatcher WW, Santos JEP. Carryover effect of postpartum inflammatory diseases on developmental biology and fertility in lactating dairy cows. *J Dairy Sci* 2016; **99**:2201–2220.
37. Moore SG, Fair T, Lonergan P, Butler ST. Genetic merit for fertility traits in Holstein cows: IV. Transition period, uterine health, and resumption of cyclicity. *J Dairy Sci* 2014; **97**:2740–2752.
38. Drackley JK. Biology of dairy cows during the transition period: the final frontier? *J Dairy Sci* 1999; **82**:2259–2273.
39. Allen MS, Bradford BJ, Oba M. Board-invited review: The hepatic oxidation theory of the control of feed intake and its application to ruminants. *J Anim Sci* 2009; **87**:3317–3334.
40. McCabe M, Waters S, Morris D, Kenny D, Lynn D, Creevey C. RNA-seq analysis of differential gene expression in liver from lactating dairy cows divergent in negative energy balance. *BMC Genomics* 2012; **13**:193.
41. Moran B, Cummins SB, Creevey CJ, Butler ST. Transcriptomics of liver and muscle in Holstein cows genetically divergent for fertility highlight differences in nutrient partitioning and inflammation processes. *BMC Genomics* 2016; **17**:603.
42. McCarthy SD, Waters SM, Kenny DA, Diskin MG, Fitzpatrick R, Patton J, Wathes DC, Morris DG. Negative energy balance and hepatic gene expression patterns in high-yielding dairy cows during the early postpartum period: a global approach. *Physiol Genomics* 2010; **42A**:188–199.
43. Llewellyn S, Fitzpatrick R, Kenny DA, Patton J, Wathes DC. Endometrial expression of the insulin-like growth factor system during uterine involution in the postpartum dairy cow. *Domest Anim Endocrinol* 2008; **34**:391–402.
44. Wathes DC, Cheng Z, Fenwick MA, Fitzpatrick R, Patton J. Influence of energy balance on the somatotrophic axis and matrix metalloproteinase expression in the endometrium of the postpartum dairy cow. *Reproduction* 2011; **141**:269–281.
45. MacLean JA, Chakrabarty A, Xie S, Bixby JA, Roberts RM, Green JA. Family of Kunitz proteins from trophoblast: Expression of the trophoblast Kunitz domain proteins (TKDP) in cattle and sheep. *Mol Reprod Dev* 2003; **65**:30–40.
46. Oliveira LJ, Hansen PJ. Deviations in populations of peripheral blood mononuclear cells and endometrial macrophages in the cow during pregnancy. *Reproduction* 2008; **136**:481–490.
47. Mansouri-Attia N, Oliveira LJ, Forde N, Fahey AG, Browne JA, Roche JF, Sandra O, Reinaud P, Lonergan P, Fair T. Pivotal role for monocytes/macrophages and dendritic cells in maternal immune response to the developing embryo in cattle. *Biol Reprod* 2012; **87**:123–123.
48. Kamat MM, Vasudevan S, Maalouf SA, Townson DH, Pate JL, Ott TL. Changes in myeloid lineage cells in the uterus and peripheral blood of dairy heifers during early pregnancy. *Biol Reprod* 2016; **95**:68–68.
49. Fair T. The contribution of the maternal immune system to the establishment of pregnancy in cattle. *Front Immunol* 2015; **6**:7.
50. Straszewski-Chavez SL, Abrahams VM, Mor G. The role of apoptosis in the regulation of trophoblast survival and differentiation during pregnancy. *Endocr Rev* 2005; **26**:877–897.
51. Mills CD, Kincaid K, Alt JM, Heilman MJ, Hill AM. M-1/M-2 Macrophages and the Th1/Th2 Paradigm. *J Immunol* 2000; **164**:6166–6173.
52. Martinez FO, Gordon S. The M1 and M2 paradigm of macrophage activation: time for reassessment. *F1000Prime Rep* 2014; **6**:12703.
53. Mantovani A, Sozzani S, Locati M, Allavena P, Sica A. Macrophage polarization: tumor-associated macrophages as a paradigm for polarized M2 mononuclear phagocytes. *Trends Immunol* 2002; **23**:549–555.
54. Smith SK. Angiogenesis, vascular endothelial growth factor and the endometrium. *Hum Reprod Update* 1998; **4**:509–519.
55. Ushio-Fukai M, Alexander RW. Reactive oxygen species as mediators of angiogenesis signaling Role of NAD(P)H oxidase. *Mol Cell Biochem* 2004; **264**:85–97.
56. Nguyen T, Nioi P, Pickett CB. The Nrf2-antioxidant response element signaling pathway and its activation by oxidative stress. *J Biol Chem* 2009; **284**:13291–13295.
57. Galvan-Pena S, O'Neill LAJ. Metabolic reprograming in macrophage polarization. *Front Immunol* 2014; **5**:420.
58. Baitsch D, Bock HH, Engel T, Telgmann R, Muller-Tidow C, Varga G, Bot M, Herz J, Robenek H, von Eckardstein A, Nofer J-R. Apolipoprotein E induces antiinflammatory phenotype in macrophages. *Arterioscler Thromb Vasc Biol* 2011; **31**:1160–1168.
59. Wang N, Liang H, Zen K. Molecular mechanisms that influence the macrophage M1-M2 polarization balance. *Front Immunol* 2014; **5**:614.
60. Poralla L, Stroh T, Erben U, Sittig M, Liebig S, Siegmund B, Glauben R. Histone deacetylase 5 regulates the inflammatory response of macrophages. *J Cell Mol Med* 2015; **19**:2162–2171.
61. Perišić Nanut M, Sabotič J, Jewett A, Kos J. Cysteine cathepsins as regulators of the cytotoxicity of NK and T cells. *Front Immunol* 2014; **5**:616.

62. Song G, Bazer FW, Spencer TE. Differential expression of cathepsins and cystatin C in ovine uteroplacental tissues. *Placenta* 2007; **28**:1091–1098.
63. Song G, Bailey DW, Dunlap KA, Burghardt RC, Spencer TE, Bazer FW, Johnson GA. Cathepsin B, Cathepsin L, and Cystatin C in the porcine uterus and placenta: Potential roles in endometrial/placental remodeling and in fluid-phase transport of proteins secreted by uterine epithelia across placental areolae. *Biol Reprod* 2010; **82**:854–864.
64. Heldin C-H, Westermark B. Mechanism of action and in vivo role of platelet-derived growth factor. *Physiol Rev* 1999; **79**:1283–1316.
65. Stanley ER, Chitu V. CSF-1 receptor signaling in myeloid cells. *Cold Spring Harb Perspect Biol* 2014; **6**:a021857–a021857.
66. Pollard JW. Trophic macrophages in development and disease. *Nat Rev Immunol* 2009; **9**:259–270.
67. Mansouri-Attia N, Aubert J, Reinaud P, Giraud-Delville C, Taghouti G, Galio L, Everts RE, Degrelle S, Richard C, Hue I, Yang X, Tian XC et al. Gene expression profiles of bovine caruncular and intercaruncular endometrium at implantation. *Physiol Genomics* 2009; **39**:14–27.
68. Bazer FW, Spencer TE, Johnson GA, Burghardt RC, Wu G. Comparative aspects of implantation. *Reproduction* 2009; **138**:195–209.
69. Gray CA, Bartol FF, Tarleton BJ, Wiley AA, Johnson GA, Bazer FW, Spencer TE. Developmental biology of uterine glands. *Biol Reprod* 2001; **65**:1311–1323.
70. Giancotti FG, Ruoslahti E. Integrin signaling. *Science* 1999; **285**:1028–1033.
71. MacIntyre DM, Lim HC, Ryan K, Kimmins S, Small JA, MacLaren LA. Implantation-associated changes in bovine uterine expression of integrins and extracellular matrix. *Biol Reprod* 2002; **66**:1430–1436.
72. Bridger PS, Haupt S, Leiser R, Johnson GA, Burghardt RC, Tinneberg H-R, Pfarrer C. Integrin activation in bovine placentomes and in caruncular epithelial cells isolated from pregnant cows. *Biol Reprod* 2008; **79**:274–282.
73. Reynolds LP, Redmer DA. Angiogenesis in the placenta. *Biol Reprod* 2001; **64**:1033–1040.
74. Valour D, Degrelle SA, Ponter AA, Giraud-Delville C, Campion E, Guyader-Joly C, Richard C, Constant F, Humblot P, Ponsart C, Hue I, Grimard B. Energy and lipid metabolism gene expression of D18 embryos in dairy cows is related to dam physiological status. *Physiol Genomics* 2014; **46**:39–56.